Adipogenic capacity and the susceptibility to type 2 diabetes and metabolic syndrome

May-Yun Wang*, Paul Grayburn†, Shuyuan Chen†, Mariella Ravazzola‡, Lelio Orci‡, and Roger H. Unger*§¶

*Touchstone Center for Diabetes Research, University of Texas Southwestern Medical Center, Dallas, TX 75390-8854; §Veterans Affairs Medical Center, Dallas, TX 75216; †Baylor University Medical Center, Dallas, TX 75226; and ‡Department of Cell Physiology and Metabolism, University Medical Center, CH-1211 Geneva 4, Switzerland

Contributed by Roger H. Unger, February 27, 2008 (sent for review November 28, 2007)

To determine whether adipocyte storage capacity influences the onset and severity of type 2 diabetes and other components of the metabolic syndrome, we made normal and *db/db* mice resistant to obesity by overexpressing leptin receptor-b on the *aP2-Lepr-b* promoter. On a 4% diet, these mice have no phenotype, but on a 60% fat diet, they resist diet-induced obesity because constitutive adipocyte-specific overexpression of Lepr-b prevents obesity via the antilipogenic autocrine/paracrine action of leptin on adipocytes. After 8 months on the same 60% fat diet, body fat of transgenic mice was 70% below WT controls. Cardiac and liver fat was elevated in the transgenics, and their hyperinsulinemia was more marked, suggesting greater insulin resistance. The *aP2-Lepr-b* transgene also prevented obesity in *db/db* mice; at 10 weeks of age their body fat was half that of the *db/db* mice. This lack of obesity was attributable to reduced expression of sterol regulatory element binding protein-1c and its target lipogenic enzymes in adipose tissue and a 6-fold increase in Pref-1 mRNA. Severe diabetes was present in transgenics at 4 weeks of age, 10 weeks before db/db controls. Echocardiographic evidence of cardiomyopathy appeared at 10 weeks, weeks before the *db/db* mice. Histologically, loss of β cells and myocardial fibrosis was present in the transgenic group at least 6 weeks before the *db/db* mice. These results suggest that the expression level of genes that regulate the adipogenic response to overnutrition profoundly influences the age of onset and severity of diet-induced type 2 diabetes and co-morbidities.

adipogenesis | apoptosis | lipotoxicity | Pref-1 | leptin

Fifty million Americans now carry the diagnosis of metabolic syndrome (1), a cluster of life-shortening morbidities that includes type 2 diabetes (T2D) (2). The temporal relationship between a change in the caloric environment in the U.S. and the first recognition of the syndrome in 1981 is evidence of a crucial environmental role, whereas individual differences in susceptibility to the chronic caloric excess imply an important genetic input. Whereas many genes may influence the susceptibility to caloric excess, genes of adipogenesis are particularly attractive candidates for two reasons. First, in both rodents and humans, lipids have been shown to accumulate in the organs that are most affected in metabolic syndrome (3, 4). Second, ectopic lipid overload has been demonstrated to disable and destroy normal cardiomyocytes (5) and pancreatic β cells (6) through the process of lipoapoptosis (7). Therefore, it follows that, during sustained overnutrition, the capacity of adipose tissue to store the surplus lipids that might otherwise damage important organs would determine the overflow of lipids into nonadipocytes. Indeed, when adipocytes are deficient, as in generalized congenital lipodystrophy, the metabolic syndrome appears at an earlier age and is more severe than in the obesity-associated counterpart.

To determine the influence of adipogenesis on an environmentally induced form of metabolic syndrome, we have produced a transgenic mouse model in which the adipocytes seem to be normal on a normal diet but do not undergo normal hypertrophy and hyperplasia on a high fat diet. The transgene, the full-length leptin receptor on an aP2 promoter (Lepr-b), prevents the disappearance of adipocyte Lepr-b that normally accompanies overfeeding and that is essential to block the antilipogenic autocrine action of leptin that prevents fat storage (8). We speculated that the persistent constitutive expression of Lepr-b on adipocytes during long-term overnutrition would result in lipid spillover into nonadipose organs and thereby cause manifestations of the metabolic syndrome, such as hepatic steatosis and insulin resistance, to appear.

If, indeed, this scenario were the case, it would imply that the predisposition to metabolic syndrome is inversely related to the adipogenic response to overnutrition. This notion would fit well with the report of Ruderman *et al*. that "metabolically obese, normal weight" patients with metabolic syndrome tend to be younger than those with overt obesity (9). It would also fit with the demonstration by Kim *et al*. that further expansion of the fat mass of congenitally obese mice improves their metabolic profile (10). Using this model of restricted adipogenesis, we observed that the level of adipogenesis is a key determinant of both age of onset and severity of the metabolic syndrome in both normal mice and in *db/db* mice with an inherited predisposition to severe obesity-associated metabolic syndrome caused by a mutation in the leptin receptor-b (Lepr-b) (11). Thus, contrary to popular belief, obesity protects, at least temporarily, against T2D and metabolic syndrome by buffering the effects of overnutrition on ectopic lipid deposition.

Results

aP2-Lepr-b Transgene Increases Ectopic Lipid Deposition During High Fat Feeding. To determine the influence of adipogenic capacity on the metabolic consequences of overnutrition, normal WT mice and aP2-Lepr-b transgenic mice were placed on a diet containing either 4% or 60% fat for 8 months, and various metabolic parameters were compared. There were no differences in food intake on either diet. On the 4% fat diet, no intergroup differences in body weight or body fat were evident over the 8-month period of observation (Table 1, 4% fat diet). Except for a modest but statistically significant increase in plasma triglyceride levels, none of the metabolic parameters measured differed from WT mice (Table 1, 4% fat diet).

However, on the 60% fat diet for 8 months, marked differences between the two groups appeared despite almost identical food intakes. The body fat of the transgenic mice was 70% less than the WT controls reflecting severe impairment of adipogenesis (Table 1, 60% fat diet). Ectopic triacylglycerol (TAG) deposition was significantly greater in the heart and liver of the transgenic mice.

Author contributions: R.H.U. designed research; M.-Y.W. performed research; P.G., S.C., M.R., and L.O. contributed new reagents/analytic tools; M.R. and L.O. analyzed data; and R.H.U. wrote the paper.

The authors declare no conflict of interest.

¶To whom correspondence should be addressed at: University of Texas Southwestern Medical Center, 5323 Harry Hines Boulevard, L5.202, Dallas, TX 75390-8854. E-mail: roger.unger@utsouthwestern.edu.

This article contains supporting information online at www.pnas.org/cgi/content/full/0801981105/DCSupplemental.

© 2008 by The National Academy of Sciences of the USA

MEDICAL SCIENCES

Table 1. Metabolic parameters of WT and transgenic (tg) (N = 6) mice fed 4% or 60% fat diets for 8 months

	4% fat diet			60% fat diet		
Measurement	WT	*P* value (WT vs. tg)	tg	WT	*P* value (WT vs. tg)	tg
Body weight, g	36.8 ± 2.6	NS	33.2 ± 2.6	67.3 ± 1.1	0.00008	36.2 ± 3.8
Food intake, g	4.3 ± 0.4	NS	4.1 ± 0.4	3.6 ± 0.2	NS	3.9 ± 0.5
Body fat, g	5.3 ± 0.4	NS	4.8 ± 0.5	27.5 ± 0.8	0.00002	8.4 ± 2.0
Fasting blood glucose, mg/dl	70.3 ± 9.6	NS	82.3 ± 9.1	103.5 ± 16.3	0.015	154.5 ± 4.5
Blood glucose, mg/dl	146.5 ± 35.5	NS	161.7 ± 4.4	184.6 ± 30.5	NS	189.2 ± 31.8
Insulin, ng/ml	1.710 ± 0.28	NS	1.232 ± 0.087	3.927 ± 2.212	0.008	11.024 ± 0.9
Leptin, ng/ml	2.32 ± 0.69	NS	4.38 ± 2.28	216.0 ± 33.3	0.015	13.75 ± 6.75
TAG, mg/dl	109 ± 1.3	0.01	131.7 ± 3.8	127.8 ± 39.8	NS	105.4 ± 35.1
FFA, mM	0.142 ± 0.02	NS	0.114 ± 0.019	0.204 ± 0.006	0.09	0.255 ± 0.038
Liver weight, g	1.92 ± 0.15	NS	1.86 ± 0.42	2.29 ± 0.18	NS	3.02 ± 0.49
Heart weight, g	0.15 ± 0.01	NS	0.16 ± 0.013	0.15 ± 0.005	0.018	0.23 ± 0.03
Liver TAG, mg/g	42.6 ± 3.1	NS	49.0 ± 9.1	130.62 ± 8.77	0.032	177.65 ± 15.01
Heart TAG, mg/g	4.29 ± 1.94	NS	3.16 ± 2.55	4.17 ± 0.81	0.055	9.66 ± 2.00
Muscle TAG, mg/g	14.42 ± 5.23	NS	17.32 ± 6.75	28.34 ± 3.28	NS	23.07 ± 0.77
Pancreas TAG, mg/g	3.31 ± 0.51	NS	4.85 ± 2.28	24.39 ± 7.12	NS	22.97 ± 2.07

NS, Nonsignificant ($P > 0.055$).

The hearts appeared larger and this increase in size was reflected by a significant increase in organ weight (Table 1, 60% fat diet). However, in skeletal muscle, the differences in TAG content of WT and tg groups, although significantly higher than on a 4% fat diet, did not significantly differ from each other (Table 1, 60% fat diet). Postprandial insulin levels were almost three times higher in the transgenic mice than in controls, despite comparable mild elevation in postprandial glucose concentrations (Table 1, 60% fat diet). This increase is consistent with insulin resistance.

aP2-Lepr-b Transgene Prevents Genetic Obesity in *db/db* Mice. To determine whether the aP2-Lepr-b transgene would also prevent genetic obesity in *db/db* mice, a well characterized model of hyperphagia, obesity and T2D, we derived transgenic *db/db*-aP2-Lepr-b (*db/db*-tg) mice. Lepr-b protein was detected in the fat tissue of *db/db*-tg mice but not in *db/db* mice (Fig. 1*B*).

Both *db/db* and *db/db*-tg mice were fed a chow diet containing 6% fat for 10 weeks and were equally hyperphagic. Their food intake during that period was virtually identical (5.1 vs. 5.3 g/d), exceeding by ≈48% the food intake of normal WT C57BL/6 mice (Table 2).

In contrast to the *db/db* mice, *db/db-tg* mice did not become obese. At 10 weeks, their body weight averaged only 55% of the *db/db* mice (28.5 ± 5.8 g vs. 51 ± 3.4 g; $P = 0.0007$), and they were not significantly heavier than the normal WT controls (Table 2). The body fat of *db/db*-tg mice was less than half of *db/db* mice (Table 2 and Fig. 1*A*). Microscopically, the adipocyte diameter in the *db/db-tg* mice averaged 25 ± 5 μm, compared with 55.3 ± 8 μm in the *db/db* mice ($P < 0.0001$) (Fig. 1*B*). The adipose tissue content of P-STAT3, a marker of leptin receptor-mediated action, was increased in the transgenic mice (Fig. 1*C*), indicating that differences in the adipose tissue of lean *db/db*-tg mice were likely transduced via the transgenic Lepr-b.

aP2-Lepr-b Transgene Accelerates the Development of Diabetes. In the *db/db* mice at 10 weeks of age, ≈6 weeks after the onset of obesity (Fig. 2*A*), nonfasting blood glucose levels were still relatively normal, averaging 175 ± 42 mg/dl. By contrast, most of the nonobese *db/db*-tg mice had become overtly diabetic by 5 weeks of age. At 10 weeks of age, all were severely diabetic, with a mean glucose level of 574 ± 15 mg/dl. They were all obviously ill, with severe polyuria (Fig. 2*B*), polydipsia (Fig. 2*C*), and glycosuria (Fig. 2*D*), whereas all *db/db* mice were still normal clinically at this time point, with a mean nonfasting glucose level of <200 mg/dl (175 ± 42).

To determine whether the earlier onset and greater severity of T2D in the *db/db*-tg mice resulted from a greater loss of β cells, their pancreata were stained for insulin and glucagon. At 10 weeks of age, β cells of the *db/db*-tg mice were profoundly reduced in both number and area (Fig. 3*A*), and severe derangement of islet

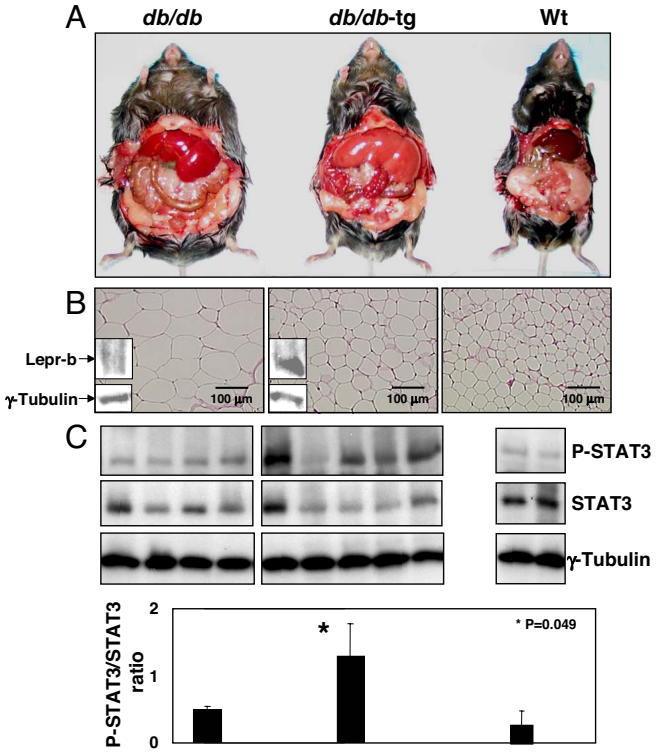

Fig. 1. Comparison of 10-week-old *db/db*, *db/db*-tg, and normal mice. (*A*) Exposure of s.c. and visceral fat showing less fat in the *db/db*-tg mouse. Appearance of both *db/db* and *db/db*-tg livers suggests steatosis, which is more marked in the latter. (*B*) Sections of epididymal fat of *db/db*, *db/db*-tg, and WT mice, showing reduced size of *db/db*-tg adipocytes compared with *db/db* despite identical food intake (Table 2). Immunoblot for C terminus of mouse Lepr-b is positive in *db/db*-tg fat but not in *db/db* fat. (*C Upper*) Adipose tissue phospho-STAT3, an index of leptin action, in *db/db*, *db/db*-tg, and normal mice. (*Lower*) Bars indicate the mean ± SEM of phospho-STAT3/STAT3 ratios.

Table 2. Metabolic profiles of 10-week-old WT, *db/db*, and *db/db*-tg (N = 4) mice fed 6% fat diet

Measurement	WT	*P* value (WT vs. *db/db*)	*db/db*	*P* value (*db/db* vs. *db/db*-tg)	*db/db*-tg
Body weight, g	30.9 ± 1.0	0.0002	51.1 ± 3.4	0.0007	28.5 ± 5.8
Food intake, g	3.5 ± 0.5	0.05	5.1 ± 0.5	0.836	5.3 ± 0.6
Body fat, g	8.49 ± 1.38	0.0001	24.38 ± 2.83	0.004	11.25 ± 4.09
Adipocyte diameter, μm	17.4 ± 1.4	4.2E−13	55.3 ± 7.9	7.8E−12	25.0 ± 4.5
Fasting blood glucose, mg/dl	77.6 ± 7.9	0.059	106.4 ± 29.3	0.0002	271.0 ± 31.2
Blood glucose, mg/dl	130.0 ± 16.7	0.734	175.0 ± 42.0	0.002	574.5 ± 14.5
Urine glucose, mg/dL	negative		negative		>2,000
Insulin, ng/ml	1.849 ± 0.66	0.018	12.990 ± 5.30	0.068	5.778 ± 0.742
Leptin, ng/ml	1.47 ± 0.26	0.0014	9.19 ± 1.17	0.0009	3.59 ± 1.46
TAG, mg/dl	23.2 ± 4.1	0.029	50.7 ± 5.5	0.281	62.4 ± 15.1
FFA, mM	0.166 ± 0.033	0.0008	0.848 ± 0.198	0.229	0.694 ± 0.117
Liver TAG, mg/g	29.2 ± 0.44	0.0002	59.4 ± 2.65	0.097	96.9 ± 4.42
Heart TAG, mg/g	5.2 ± 0.63	0.936	5.3 ± 0.75	0.02	7.43 ± 0.75
Muscle TAG, mg/g	17.2 ± 3.98	0.432	23.4 ± 7.37	0.019	49.4 ± 6.58
Pancreas TAG, mg/g	2.70 ± 0.28	0.038	23.0 ± 8.89	0.065	6.83 ± 2.34

organization was apparent (Fig. 3*B*). By contrast, islet organization in the *db/db* mice was still perfectly preserved. The volume density of the insulin-positive β cells was 0.053 ± 0.01 in pancreas sections of *db/db* mice (area evaluated 30.8 mm^2, three animals) compared with 0.011 ± 0.007 in the *db/db*-tg mice (area evaluated 27.4 mm^2, three animals) (Fig. 3*B*).

In addition, there were differences in the distribution of glucagon-positive α cells. In *db/db* mice, they were arrayed peripherally as in normal islets (12), whereas in *db/db*-tg mice they were found in increased proportion and had lost their characteristic peripheral distribution within the islets (Fig. 3*C*).

Quantitative Relationship of Adipocyte Lepr-b Expression to Adiposity and Diabetes. If the aP2-Lepr-b transgene is the cause of the foregoing differences in adipogenesis, ectopic lipid deposition, and glucose metabolism, one would expect to find a relationship between its expression level and the adipogenic capacity and the blood glucose level. To test for this relationship, we divided the *db/db*-tg mice into high and low expressors of adipocyte aP2-Lepr-b. At 18 weeks of age, the body weight of the high expressors averaged only 27.6 ± 1.3 g, compared with 44.7 ± 1.8 g in the low expressors. Body fat measured 9.1 ± 0.6 g in the high expressors and 13.8 ± 0.8 g in the low group (P = 0.03), evidence that the expression level of this transgene influences adipogenesis.

To determine whether the level of expression of Lepr-b on adipocytes is a factor in the development of diabetes, we compared the nonfasting blood glucose levels and insulin levels in the two groups at 18 weeks of age. In the low expressors, glucose and insulin levels averaged 207 ± 44 mg/dl and 25 ± 7 ng/ml, respectively, compared with 577 ± 30 mg/dl and 15 ± 5 ng/ml in the high expressors ($P < 0.05$) (data not shown). Although the difference was not statistically significant, the lower insulin levels in the high expressors, despite greater hyperglycemia, are consistent with more severe β cell destruction.

aP2-Lepr-b Transgene Accelerates Lipotoxic Heart Disease of *db/db*-tg Mice. Ectopic fat deposition has been identified in the heart and other organs of obese rodents (3, 13, 14), suggesting that lipotoxic cardiomyopathy may be a genuine disease entity (5, 15). Ectopic fat deposition has also been identified in humans with metabolic syndrome, and, in human obesity, myocardial fat has been implicated in certain cardiac derangements (4). To determine whether there is a relationship between adipogenic capacity and cardiac function, transthoracic echocardiograms were obtained in the nonobese *db/db*-tg and obese *db/db* mice at 10 weeks of age. The impairment in systolic function and depression of fractional shortening was greater in the former (Fig. 4*A*). Postmortem studies at 10 weeks of age showed the hearts of *db/db*-tg mice to be markedly enlarged (Fig. 4*B*) and their cardiac TAG content 29% higher than the *db/db* mice (P = 0.02) (Table 2).

Morphologic examination of the hearts of *db/db*-tg mice revealed disruption of their myocardial architecture and replacement of myofibers by fibrous tissue (Fig. 4*C*). Thus, severe lipotoxic cardiomyopathy occurred at an earlier age in mice with a restricted adipogenic capacity.

Effects of the aP2-Lepr-b Transgene on Lipid Deposition in Other Organs of *db/db* Mice. To determine the effect of a reduced adipogenic capacity during overnutrition on ectopic lipid deposition in other organs, we compared the TAG content of the liver, pancreas, and skeletal muscle of *db/db* and *db/db*-tg mice. The hepatic TAG content of the *db/db*-tg mice was 61% higher than in the *db/db* group [nonsignificant (NS)] and over three times that of normal WT mice. The gastrocnemius muscle TAG content was more than twice that of *db/db* ($P < 0.02$), and almost three times the normal value. Pancreatic TAG content was above normal in both *db/db* and *db/db*-tg mice but, unexpectedly, was higher in the former. Plasma TAG levels of *db/db*-tg mice, which were almost three times normal values, were only slightly above those of *db/db* mice (N.S.) (Table 2).

Expression Profiles in Adipose Tissue. The ectopic lipid deposition of the *db/db*-tg mice reflects a diminished capacity of adipocytes to store unoxidized fatty acids, either because of impaired lipogenesis and/or a diminished capacity for hypertrophy and/or proliferation. We therefore determined by quantitative real-time RT-PCR the expression level of relevant genes involved at various levels in these processes (Table 3). The expression of the lipogenic transcription factor, sterol regulatory element-binding protein (SREBP)-1c, was reduced, together with its target enzymes of fatty acid synthesis and esterification, acetyl CoA carboxylase (ACC)-α and -β, fatty acid synthetase, and glycerol phosphate acyl transferase (GPAT) and diacylglycerol acyl transferase (DGAT)-1. Importantly, there was a 6-fold increase in the mRNA of preadipocyte factor (Pref)-1, an inhibitor of adipogenesis that is expressed on preadipocytes but not on adipocytes (16). These results suggest that a block of lipogenesis and adipocyte maturation caused the obesity resistance and ectopic lipid deposition.

There was also evidence of increased fatty acid oxidation in adipocytes of the *db/db*-tg mice, as we had reported (8). The mRNA of the peroxisomal enzyme acyl CoA oxidase (ACO) was increased, and the decreased expression of both ACC isoforms would be

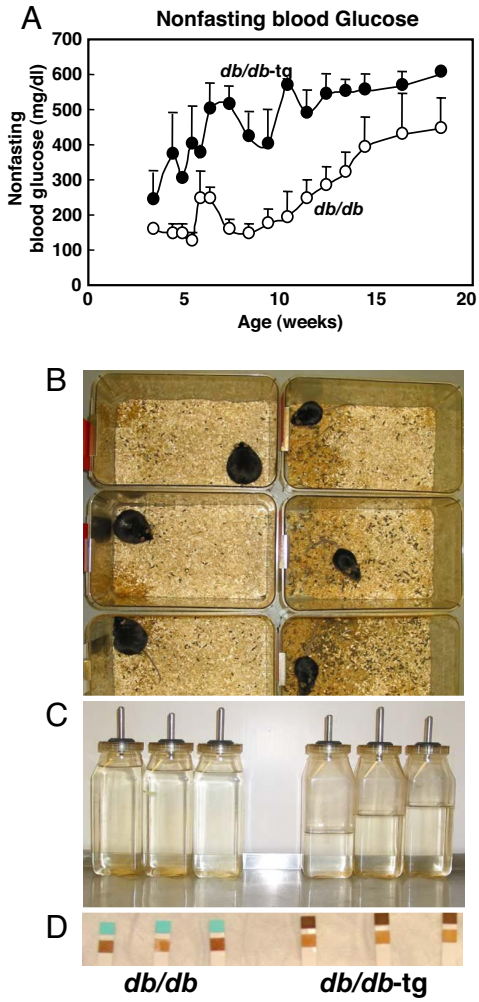

Fig. 2. Clinical evidence that obesity delays the onset of T2D in *db/db* mice. (*A*) Comparison of nonfasting blood glucose levels in obese *db/db* and nonobese *db/db*-tg mice, demonstrating the later appearance of less severe hyperglycemia in the *db/db* mice. (*B* and *C*) Comparison of the cages and the water bottles of 10-week-old obese *db/db* and nonobese *db/db*-tg mice, showing evidence of polyuria and polydipsia only in the latter. (*D*) Comparison of urine glucose testing in obese *db/db* and nonobese *db/db*-tg mice (Keto-Diastix Reagent Strip, Bayer, Elkhart, IN), showing glycosuria only in the latter.

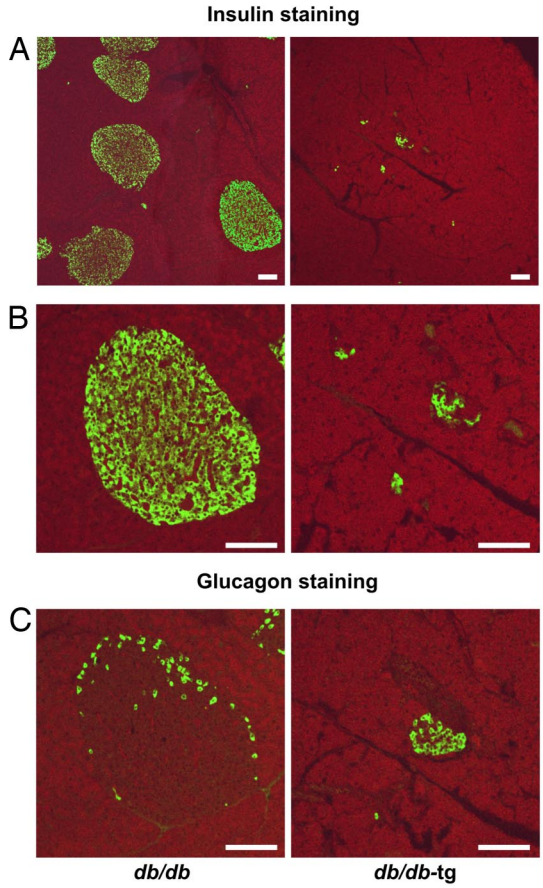

Fig. 3. Immunofluorescent staining for insulin and glucagon of pancreas. (*A*) Low magnification view of pancreatic tissue showing a large number of islets in *db/db* mice (*Left*) and a fewer number of small insulin-positive areas in *db/db*-tg mice (*Right*). (*B*) Higher magnification of the cells in *A*. (*C*) The normal topography of glucagon-containing α cells in *db/db* mice (*Left*) contrasts with disrupted cells in *db/db*-tg mice (*Right*). (Scale bars: 100 μm.)

expected to reduce malonyl-CoA-mediated inhibition of carnitine palmitoyl CoA transferase (CPT)-1. Further, a 7-fold higher ratio of phosphorylated to total AMP-activated protein kinase (0.7 ± 0.4 vs. 0.1 ± 0.004; $P = 0.05$) (data not shown) suggested increased mitochondrial oxidation of fatty acids. Finally, expression of peroxisome proliferator-activated receptor-γ coactivator (PGC)-1α, an up-regulator of mitochondrial biogenesis (17), was increased in the fat of *db/db*-tg mice, presumably expanding its oxidative capacity. Whereas increased fatty acid oxidation could have contributed to the obesity resistance of the *db/db*-tg mice, it was not sufficient to prevent the ectopic lipid overflow in the *db/db*-tg mice.

Because of the putative role of inflammation in obesity and metabolic syndrome, we compared various inflammatory markers in the adipose tissue, liver, and muscle of the *db/db* and *db/db*-tg mice. At 10 weeks of age, there were no statistically significant differences in IL-1β, IL-6, TNF-α, or macrophage chemoattractant protein-1 (MCP-1) mRNA in the three tissues. Serum amyloid A (SAA-1) mRNA was significantly higher in skeletal muscle of *db/db*-tg mice ($P = 0.026$) but not in fat or liver tissue; however, plasma SAA did not differ in the two groups (data not shown). C-reactive protein was increased in the liver of *db/db*-tg mice ($P = 0.05$). In contrast to the increase in phosphorylated AMP kinase in the fat tissue of *db/db*-tg mice, there were no differences in liver or muscle (data not shown). The comparison of expression levels of inflammatory factors appears in supporting information (SI) Table S1.

Discussion

The aim of the present study was to determine the relationship between adipocyte storage capacity and two major components of the metabolic syndrome in rodents, T2D, and lipotoxic cardiomyopathy (14). It has long been accepted that the primary function of adipocytes is to store fuel for distribution to nonadipose tissues in times of need, as during a famine (18). The present study suggests a second function of adipocytes, namely, the compartmentalization into adipocytes of the surplus calories consumed during overnutrition so as to protect nonadipose organs from lipid-induced trauma (3). Indeed, the recent demonstration by Kim *et al.* (10) that expansion of the fat mass of congenitally obese mice improves their metabolic profile lends further credence to the idea. To test this hypothesis, we studied the effects of preventing adipocyte expansion on the complications of diet-induced obesity in otherwise normal C57BL/6 mice, and in the genetic obesity of *db/db* mice.

Comparison of WT C57BL/6 controls and the aP2-Lepr-b-tg mice revealed no significant differences in ectopic lipid deposition after 8 months on a 4% fat diet. However, after 8 months of a 60%

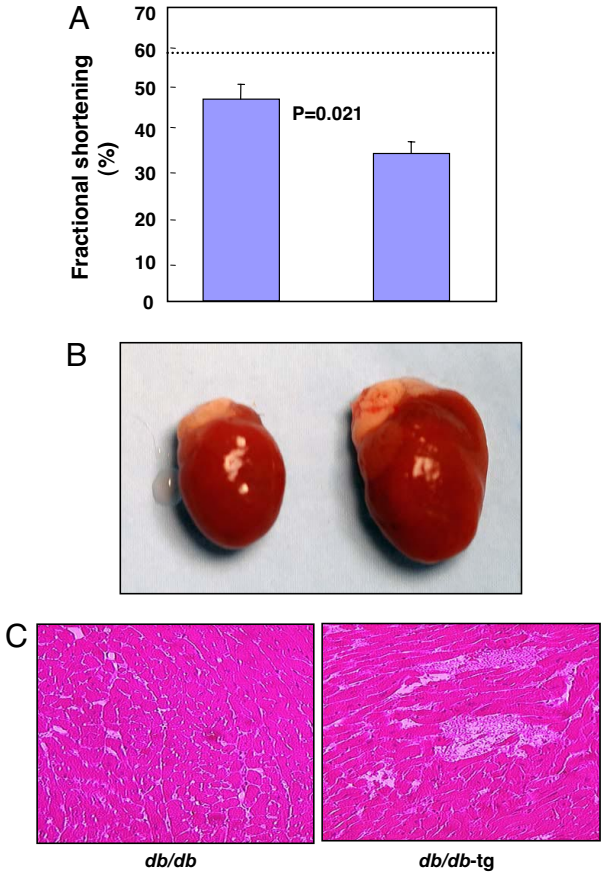

Fig. 4. Function and gross and microscopic appearance of the heart of 10-week-old *db/db* and *db/db*-tg mice. (*A*) Echocardiographically measured fractional shortening demonstrating greater functional loss in 10-week-old *db/db*-tg mice. The dotted line marks the normal value of fractional shortening. (*B*) Gross enlargement of the heart in a *db/db*-tg mouse. (*C*) Myocardium of *db/db* and *db/db*-tg mice exhibits myofiber disruption and focal fibrosis in the latter.

fat diet, the WT control mice had developed diet-induced obesity, whereas the aP2-Lepr-b-tg mice remained nonobese. The latter mice exhibited greater lipid deposition in the liver and heart. The heart was enlarged and heavier (Table 1, 60% fat diet). Both groups were hyperinsulinemic, but the hyperinsulinemia of the tg mice was approximately three times that of the WT controls, with a similar moderate elevation in nonfasting glucose levels (Table 1, 60% fat diet). But in tg mice, the difference in insulin between the 4% fat diet and the 60% fat diet was 9.8 ng/ml compared with only 2.2 ng/ml in the WT control mice (Table 1). Given the similar levels of hyperglycemia, this difference in insulin was consistent with greater insulin resistance in the tg group.

As expected, comparison of genetically obese WT *db/db* mice with slender *db/db* mice expressing the aP2-Lepr-b transgene revealed a far greater impact of restricted adipogenesis. In the former mice, the metabolic syndrome follows the onset of obesity by ≈7 weeks, or ≈12 weeks of age. Blood glucose levels remain <200 mg/dl until that time (Fig. 2*A*), evidence that their β cells are still delivering enough insulin to meet the demands of rising insulin resistance. By contrast, nonobese *db/db*-tg mice enjoyed no such prediabetic "honeymoon" period. Some were seriously ill at 4–5 weeks of age, with glucose levels averaging >400 mg/dl, a level not attained by *db/db* mice until ≈14 weeks of age. All *db/db*-tg mice exhibited polyuria, polydipsia, glycosuria, and severe hyperglycemia by 10 weeks of age, consistent with the profound depletion of their β cells. Similarly, myocardial dysfunction and dilated cardiomyopathy and echocardiographic evidence of severe functional loss appeared in the *db/db*-tg mice at 10 weeks of age, whereas at 18 weeks functional loss was still minimal in the *db/db* group (Fig. 4*A*).

Table 3. Quantitative PCR analysis of mRNAs in the adipocyte tissue of *db/db* and *db/db*-tg mice using 36B4 as the invariant control

Genes	*db/db*-tg (n = 5)	*P* value
AMPKα1	0.39 ± 0.23	0.049
PPARα	0.06 ± 0.02	0.036
PGC1α	2.06 ± 0.02	0.042
SREBP-1c	0.62 ± 0.12	0.034
Pref-1	6.44 ± 0.97	0.019
IR	1.55 ± 0.04	0.043
IRS2	2.24 ± 0.50	0.018
ACO	2.26 ± 0.84	0.028
ACCα	0.51 ± 0.13	0.043
ACCβ	0.44 ± 0.04	0.041
FAS	0.23 ± 0.12	0.005
GPAT	0.36 ± 0.05	0.0003
DGAT1	0.35 ± 0.29	0.038
Leptin	0.41 ± 0.02	0.028
Resistin	0.36 ± 0.14	0.032
Adiponectin	0.70 ± 0.09	0.025

Values in *db/db*-tg mice are expressed as fold difference from *db/db* mice. No significant differences were found in the expression of the following genes: AMPKα2, PPARγ, LXRα, RXRα, C/EBPα, C/EBPβ, C/EBPδ, ChREBP, Insig-1, FOXO1, FOXC2, IRS1, CPT1, DGAT2, MCD, SCD, SOCS3, TNFα, IL-6, IL-1β, CRP, MCP-1, SAA-1, UCP1, UCP2, and UCP3.

Given the known lipoapoptotic action of lipid excess on β cells *in vitro* (7) and *in vivo* (6) and on cardiomyocytes *in vivo* (5), a lipotoxic etiology for the observed organ damage seemed plausible, particularly because there was no obvious morphologic evidence of inflammation in the tissues examined and because no increase in either TNF-α, IL-1β, IL-6, or MCP-1 expression was detected in fat, liver, or muscle tissue. However, the increase in expression of SAA-1 in skeletal muscle and CRP in liver (Table S1) makes it impossible to exclude a contributing role of inflammation in the pathogenesis of these disorders (19).

These results may have potentially important clinical implications. First, they imply that getting fat is a premetabolic syndrome manifestation, recognition of which by physicians and patients might encourage more aggressive interventions during the disease-free phase of overnutrition, rather than after the onset of overt disease, as is now customary. Elimination of the caloric surplus in uncomplicated obesity is known to prevent overt T2D in rats (20) and humans (21), evidence that premorbid intervention, long successfully used to prevent coronary artery disease, will also prevent T2D and metabolic syndrome.

Second, there are similarities between the accelerated metabolic syndrome produced transgenically in this study and the syndrome of "metabolically obese, normal weight" patients first described by Ruderman *et al.* (9). It will be of interest to determine whether their adipocyte storage capacity is subnormal, and, if so, the molecular basis of that subnormal capacity.

Third, the clear relationship between adipogenic capacity and susceptibility to T2D and metabolic syndrome raises the possibility that differences in expression or function of various adipogenic genes may influence susceptibility to diet-induced metabolic syndrome. One gene candidate for such a role is Pref-1, a secreted preadipocyte factor that inhibits adipogenesis and has been shown to exacerbate insulin resistance while preventing diet-induced obesity (H. S. Sul, personal communication). The fact that its expression was 6-fold greater in the *db/db*-tg mice than in the *db/db* mice should place it high on the list of genes that increase the ectopic deposition of lipids during chronic overeating and susceptibility for the metabolic syndrome.

Materials and Methods

Animals. C57BL/6 mice were bred locally. All were housed in individual cages in a temperature-controlled environment with 12-h light/12-h dark cycle. All mice had ad libitum access to water and pelleted mouse chow. Transgenic studies were carried out with C57BL/6 mice.

Animals were killed under anesthesia with pentobarbital sodium. Nonfasting blood samples were obtained from the inferior vena cava. All tissues were rapidly excised, frozen in liquid nitrogen, and stored at −70°C until use. Institutional guidelines for animal care and use were followed. The animal protocol was approved by the Institutional Animal Care and Research Advisory Committee of the University of Texas Southwestern Medical Center at Dallas.

Blood used for glucose determinations was collected in conscious animals by nicked tail vein bleeding between 10:00 and 12:00 a.m. Fasted blood glucose measurements were performed between 10:00 and 12:00 a.m., after food removal at 4:00 p.m. the previous day.

Transgenic Mice Production. The production of aP2-Lepr-b transgenic mice has been described in ref. 8. Briefly, mouse Lepr-b cDNA was subcloned into an expression plasmid, pSTEC-1-aP2, under the control of aP2 promoter. The resulting pSTEC-1-aP2-Lepr-b construct contained a chimeric intron derived from β-globin intron and IgG intron, and a simian virus 40 polyA addition site required for proper processing of the transgene mRNA *in vivo*. Transgenic mice were generated by microinjection of purified aP2-Lepr-b DNA fragments into pronuclei of fertilized mouse eggs, which were subsequently transferred into foster mothers. Transgenic founders and offspring were screened by PCR genotyping of genomic DNA prepared from tail biopsies with specific primers.

Generation of *aP2-Lepr-b db/db* Mice. Male heterozygous (*db*/+) mice on the C57BL/6 background (purchased from The Jackson Laboratory) were crossed with aP2-lepr-b transgenic animals that were on the same background. Double heterozygous (aP2-lepr-b *db*/+) animals were crossed again with *db*/+ to obtain aP2-lepr-b *db*/*db* genotype. Genotyping for *db*/*db* was carried out by restriction fragment-length polymorphism analysis using the enzyme RsaI on a 135-bp PCR product generated from genomic DNA isolated from these mice with the primer pair 5′-agaacggacactctttgaagtctc-3′ and 5′-cattcaaaccatagtttaggtttgtgt-3′, with 35 cycles of 94°C for 30 s, 52°C for 45 s, and 72°C for 45 s (22).

Plasma Measurements. Plasma leptin and insulin were measured by using ELISA kits (Crystal Chem, Downers Grove, IL). Plasma triglycerides were measured by using a glycerol phosphate oxidase-Trinder triglyceride kit (Sigma). Plasma-free fatty acids were measured by using the Wako NEFA kit (Wako Chemical USA, Richmond, VA).

Triacylglycerol (TAG) Content of Tissues. Mice were anesthetized with pentobarbital sodium. Tissues were rinsed with PBS (pH 7.4), dissected, and placed in liquid nitrogen immediately. Total lipids from tissues were extracted and dried under N_2 gas. TG content was assayed as described in ref. 23.

Real-Time Quantitative Polymerase Chain Reaction (RT-QPCR). Total RNA was extracted from fat tissues by TRIzol isolation method (Life Technologies, Rockville, MD). All PCRs were done in triplicate. mRNA was calculated by using the standard curve method. 36B4 RNA was used as the invariant control. Primer sequences of genes used for quantification of mRNA by RT-QPCR are shown in Table S2.

Immunoblotting. Total cell extracts prepared from fat tissues of mice were resolved by SDS/PAGE and transferred to a poly(vinylidene difluoride) membrane (Amersham Pharmacia). The blotted membrane was blocked in 1× TBS containing 0.1% Tween (TBST) and 5% nonfat dry milk (MLK) for 1 h at room temperature with gentle, constant agitation. After incubation with primary antibodies anti-phospho-STAT-3 (Tyr-705), anti-STAT-3, anti-phospho-AMPK (Thr-172), anti-AMPK (Cell Signaling Technology, Beverly, MA), anti-serum amyloid A (a gift from P. E. Scherer, University of Texas Southwestern Medical Center at Dallas) or anti-γ-tubulin (Sigma) in freshly prepared TBST-MLK at 4°C overnight with agitation, the membrane was washed twice with TBST buffer followed by incubating with goat anti-rabbit or anti-mouse HRP-conjugated IgG in TBST-MLK for 1 h at room temperature with agitation. The membrane was then washed three times with TBST buffer, and the proteins of interest on immunoblots were detected by using an enhanced chemiluminescence detection system (Amersham Pharmacia).

Islet Morphology. Pancreata were processed for immunocytochemistry as described in ref. 24 by using insulin or glucagon antibodies. The volume density of immunofluorescent cells was determined by the point counting method of Weibel (25).

Mouse Echocardiography. Transthoracic echocardiography was performed on 10-week-old mice under ketamine/xylazine anesthesia by using a 12-MHz probe as described (8, 26). Two-dimensional echocardiography in midventricular short-axis view guided left ventricular (LV) end-diastolic and end-systolic dimensions, fractional shortening, and wall thickness measurements.

Statistical Analysis. Results are presented as means ± SEM and were evaluated by using Student's *t* test for two groups.

ACKNOWLEDGMENTS. We thank J. Shelton and J. Richardson of the Molecular Pathology Core Lab at University of Texas Southwestern Medical Center for their contributions, the Scherer lab for adiponectin measurements, and Han-Yu Wang for help with genotyping. We thank P. Gorden, C. Newgard, N. Ruderman, and P. Scherer for critical review of the manuscript. We thank K. McCorkle for technical assistance with the art work, and P. McCravy for outstanding administrative assistance. This work was supported by grants from the National Institute of Diabetes and Digestive and Kidney Diseases, the Department of Veterans Affairs Merit Review, the Juvenile Diabetes Research Foundation (R.H.U.), and by the Swiss National Science Foundation (L.O.).

1. Ford ES, Giles WH, Dietz WH (2002) Prevalence of the metabolic syndrome among US adults: Findings from the third National Health and Nutrition Examination Survey. *J Am Med Assoc* 287:356–359.
2. Reaven G, Abbasi F, McLaughlin T (2004) Obesity, insulin resistance, and cardiovascular disease. *Recent Prog Horm Res* 59:207–223.
3. Lee Y, *et al*. (2001) Liporegulation in diet-induced obesity: The antisteatotic role of hyperleptinemia. *J Biol Chem* 276:5629–5635.
4. Szczepaniak LS, *et al*. (2003) Myocardial triglycerides and systolic function in humans: *In vivo* evaluation by localized proton spectroscopy and cardiac imaging. *Magn Reson Med* 49:417–423.
5. Chiu HC, *et al*. (2001) A novel mouse model of lipotoxic cardiomyopathy. *J Clin Invest* 107:813–822.
6. Lee Y, *et al*. (2007) Metabolic mechanisms of failure of intraportally transplanted pancreatic beta-cells in rats: Role of lipotoxicity and prevention by leptin. *Diabetes* 56:2295–2301.
7. Shimabukuro M, *et al*. (1998) Lipoapoptosis in beta-cells of obese prediabetic fa/fa rats: Role of serine palmitoyltransferase overexpression. *J Biol Chem* 273:32487–32490.
8. Wang MY, Orci L, Ravazzola M, Unger RH (2005) Fat storage in adipocytes requires inactivation of leptin's paracrine activity: Implications for treatment of human obesity. *Proc Natl Acad Sci USA* 102:18011–18016.
9. Ruderman N, Chisholm D, Pi-Sunyer X, Schneider S (1998) The metabolically obese, normal-weight individual revisited. *Diabetes* 47:699–713.
10. Kim JY, *et al*. (2007) Obesity-associated improvements in metabolic profile through expansion of adipose tissue. *J Clin Invest* 117:2621–2637.
11. Chen H, *et al* . (1996) Evidence that the diabetes gene encodes the leptin receptor: Identification of a mutation in the leptin receptor gene in db/db mice. *Cell* 84:491–495.
12. Orci L, Unger RH (1975) Functional subdivision of islets of Langerhans and possible role of D cells. *Lancet* 2:1243–1244.
13. Higa M, *et al*. (1999) Troglitazone prevents mitochondrial alterations, beta cell destruction, and diabetes in obese prediabetic rats. *Proc Natl Acad Sci USA* 96:11513–11518.
14. Zhou YT, *et al*. (2000) Lipotoxic heart disease in obese rats: Implications for human obesity. *Proc Natl Acad Sci USA* 97:1784–1789.
15. Unger RH, Orci L (2001) Diseases of liporegulation: New perspective on obesity and related disorders. *FASEB J* 15:312–321.
16. Wang Y, Kim KA, Kim JH, Sul HS (2006) Pref-1, a preadipocyte secreted factor that inhibits adipogenesis. *J Nutr* 136:2953–2956.
17. Wu Z, *et al* . (1999) Mechanisms controlling mitochondrial biogenesis and respiration through the thermogenic coactivator PGC-1. *Cell* 98:115–124.
18. Neel JV (1962) Diabetes mellitus: A''thrifty'' genotype rendered detrimental by ''progress''? *Am J Hum Genet* 14:353–362.
19. Shoelson SE, Lee J, Goldfine AB (2006) Inflammation and insulin resistance. *J Clin Invest* 116:1793–1801.
20. Ohneda M, Inman LR, Unger RH (1995) Caloric restriction in obese pre-diabetic rats prevents beta-cell depletion, loss of beta-cell GLUT 2 and glucose incompetence. *Diabetologia* 38:173–179.
21. Knowler WC, *et al*. (2002) Reduction in the incidence of type 2 diabetes with lifestyle intervention or metformin *N Engl J Med* 346:393–403.
22. Fiedorek FT Jr, Kay ES (1994) Mapping of PCR-based markers for mouse chromosome 4 on a backcross penetrant for the misty (m) mutation. *Mamm Genome* 5:479–485.
23. Danno H, Jincho Y, Budiyanto S, Furukawa Y, Kimura S (1992) A simple enzymatic quantitative analysis of triglycerides in tissues. *J Nutr Sci Vitaminol (Tokyo)* 38:517–521.
24. Orci L, *et al*. (1976) Hypertrophy and hyperplasia of somatostatin-containing D-cells in diabetes *Proc Natl Acad Sci USA* 73:1338–1342.
25. Weibel ER (1969) Stereological principles for morphometry in electron microscopic cytology. *Int Rev Cytol* 26:235–302.
26. Kedzierski RM, *et al*. (2003) Cardiomyocyte-specific endothelin A receptor knockout mice have normal cardiac function and an unaltered hypertrophic response to angiotensin II and isoproterenol. *Mol Cell Biol* 23:8226–8232.